

FRACTURE TOUGHNESS OF PLAIN CONCRETE UNDER MODE II LOADING

D. SUDHAKAR* AND G. APPA RAO†

*Indian Institute of Technology Madras
Chennai 600036, India
e-mail: darlasudhakar66@gmail.com

†Indian Institute of Technology Madras
Chennai 600036, India
e-mail: garao@iitm.ac.in

Keywords: Direct shear test, Modified loading setup, Plain concrete, Shear strength, Mode II fracture toughness.

Abstract: Mode II fracture behaviour plain concrete is rarely attempted due to lack of standard testing procedures. The direct shear test method is adopted to determine Mode-II fracture parameters. This paper discusses experimental investigations carried out for strength and fracture toughness of Normal, and High-strength concretes under Mode II loading. An ideal Mode II failure has been accomplished by the modified loading set-up to fail in direct shear mode. No Mode I type of failure is accompanied by the Mode II failure of the test specimen using the present modified geometry and load transfer test set-up. The experimental results have been utilized to evaluate the Mode II fracture parameters. The shear strength and Mode-II fracture toughness (K_{IIc}) increase as the compressive strength of concrete increases. The rate of loading effects the peak load and fracture toughness in shear.

1 INTRODUCTION

Concrete is widely used in construction due to its low cost, excellent compressive strength, and durability. However, it is prone to cracking under tensile or shear loading, which may lead to structural failure. Generally, shear failure in unreinforced concrete is sudden and catastrophic. Mode II failure is a standard failure mode in concrete structures subjected to shear loading. The fracture toughness of concrete under Mode II loading is a crucial parameter for characterizing the crack resistance of concrete.

Despite its importance, there is still limited understanding of the fracture toughness of plain concrete under Mode II loading due to the complexity of the testing procedures. Therefore, the present study aims to investigate the fracture toughness of plain concrete under Mode II loading using a reliable testing method and to provide insights into the behavior of

concrete under this type of loading. The Mode II types of failures also encountered in many practical situations such as shear keys, deep beams, dapped beams, short corbels, punching shear in flat slabs, bearing shoes, ledger beam bearings, and web flange stress transfer cases.

Limited standardized test methods are reported in the American or Canadian Standard (CSA) of concrete for Mode II loading. Therefore, several different test geometries such as compact shear specimens, compact cube and cylindrical, and prism specimens, double-notched cubes, double-edge notched compression test specimens, double-edge notched prisms, Iosipescu specimens, Z-type push-off specimens, four-point, and punch-through shear specimens have been investigated.

Barr and Derradj [1] conducted a numerical study on compact shear specimens and reported that tension develops at the roots of the two notches. Desai et al. [2] reported that the

Double Central Notched geometry found to be better for studies of Mode II fracture and shear strength of cementitious materials. The failure of Z-type push-off specimen is governed by splitting tension rather than shear. In Iosipescu specimen, failure is governed by Mode I or mixed mode. Numerical studies on Punch through specimen revealed that significant tensile stresses occur at the crack tip. In Double edge notched specimen, the cracks initiate in a mixed I/II mode and propagate in Mode-I.

Proposki [3] investigated the influence of water/cement ratio on fracture toughness in shear of ordinary concrete using a double-notch cube. It has been found that for lower w/c-ratios (0.55-0.70) micro cracks propagate along the grains of C_3S located in the cement gel, and for higher w/c-ratios (0.75-0.90) micro cracks propagated transgranularly in $Ca(OH)_2$ crystals and through the capillary and structural pores or along the fissures increasing in size, located on the grain boundary/cement paste interface and concluded fracture toughness of concrete decrease with the increase of water/cement ratio. Mirsayah and Banthia [4] modified the prism with a 15 mm-deep all-around notch to initiate the shear failure. Appa Rao and Sreenivasa Rao [5] performed studied with different notch and beam depths for achieving shear failure. It has been reported that the beam with 2.0 mm wide and 15mm deep all-round notch failed the beam in pure shear. Appa Rao and Sreenivasa Rao [6] conducted direct shear test on double notched prisms to determine the fracture toughness of steel fiber reinforced concrete and concluded that the addition of steel fibers in plain concrete significantly improves the fracture toughness. Mu et al. [7] conducted double-plane direct shear tests to determine the fracture parameters of Aligned fiber reinforced concrete and steel fiber reinforced concrete and concluded that the fracture properties of aligned fiber reinforced concrete was superior than fiber reinforced concrete with random fiber distribution. Sadvskaya et al. [8] investigated the influence of dispersed reinforcement on the stress intensity factor of various nanoconcrete matrices and with different dispersed reinforcement fabric. It shows that dispersed

reinforcement has a significant effect on crack resistance. The stress intensity factor increases from 74 to 150% with steel wire fiber, from 29 to 129% with steel fiber from sheet, from 14 to 131% with polymer fiber, and from 22 to 124% with polyreinforced material relative to nonreinforced nanoconcrete. Qing et al. [9] reviewed the existing methods and overviews of research findings about Aligned Fiber Reinforced Concrete (AFRC) and reported that the flexural, tensile, shear, and fracture properties of AFRC are obviously superior to those of FRC with random fiber distribution, and they have good impact resistance and explosion resistance at different strain rates.

2 MODIFIED TEST SET-UP

The Japan Society of Civil Engineering (JSCE) proposed a standard method JSCE SF-6 [10] to obtain the shear properties of FRC. Mirsayah and Banthia [4] experimented as per JSCE SF-6, but the failure plane often deviated from the narrow region under concentrated shear, which is the prescribed plane for failure, and suggested a modification to specimen with a 15 mm-deep all-round notch to predefine the crack plane, the shear failure occurred in the prescribed plane of fracture. Appa Rao and Sreenivasarao [6] modified the loading shear load set-up by applied through a loading block with two loading knife edges placed 150 mm apart. The prism was supported on another rigid block over a pair of knife edges that were 155 mm apart. Garcia et al. [11] also recommended concentrated loading set-up produces a cracking governed mainly by shear stresses and a failure that occurs within the weak area defined by the notch. Mirsayah and Banthia [4], Appa Rao and Sreenivasa Rao [6] measured the slip by two linear variable displacement transducers (LVDTs) attached to the top and bottom surfaces of the specimen, available tests set-up could not measure the slip below the failed shear plane of double edge notched prisms. Hence, in the present study the test set-up has been modified by a square steel plate (350 x 350 mm) provided with four holes to facilitate the four LVDTs attached to the bottom surface of the specimen to measure the

made in order to predefine the crack plane in the shear specimens using a diamond saw cut machine as shown in Figure 2.



Figure 2: Preparation of all-around notches

In the present test set-up, the shear load was applied by a knife edge loading block. The specimens were tested with Advantest Controls 300 kN Manually Operated Servo Hydraulic closed loop Flexure testing machine under displacement control with a displacement rate of 0.001 to 0.003mm/sec. The Servo oil pump pressure input values (k_P) entering manually throughout the experiment ($k_P = 0$ to 0.12 up to peak load, later 0.12 to 0.15). During the testing, the slip was measured with linear variable displacement transducers (LVDTs). Slip was measured along the two shear planes by averaging signals from the two linear variable displacement transducers (LVDTs) attached along each shear plane at the bottom surface of the specimen and load-displacement data were recorded at a frequency of 1 Hz.

5 RESULTS AND DISCUSSION

5.1 Compressive strength and split tensile strengths

The compressive strength of concrete was determined in accordance with IS:516-1959 by testing three cubes of 150 x 150 x 150 mm. The split tensile strength of concrete was determined according to IS: 5816 – 1999 by testing three cylinders of 150 mm diameter and 300 mm height. The average strength in compression and split tension are presented in Table 2.

5.2 Failure pattern in concrete in shear

Figures 3 and 4 shows the failed specimens of two groups of plain concrete.



Figure 3: Failure of M30-0.50-Specimen No.3

All specimens failed in pure Mode II along the shear plane coinciding with the preformed notches. No flexural cracks were observed in all the specimens. M30-0.50-S3 specimen fractured along two shear planes and broken into three pieces as shown in Figure 3.

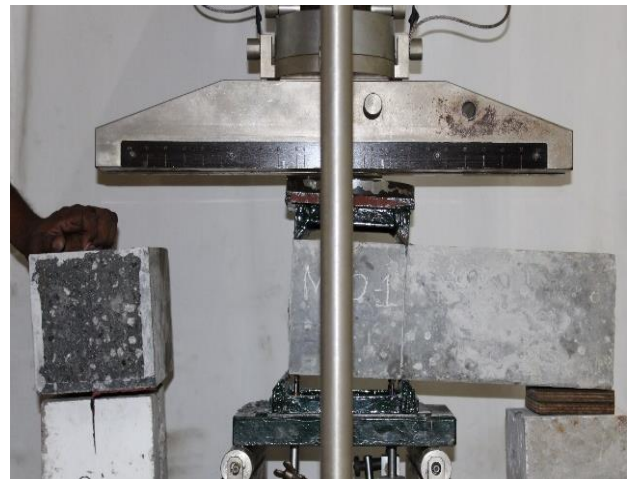


Figure 4: Failure of M70-0.32-Specimen No.1

5.3 Load-slip response

All specimens were tested under different loading rates to study the effect of loading rate on fracture parameters. Figures 5 and 6 shows typical load-slip response under direct shear. Typical load-slip responses under direct shear loading for two group of plain concrete specimens.

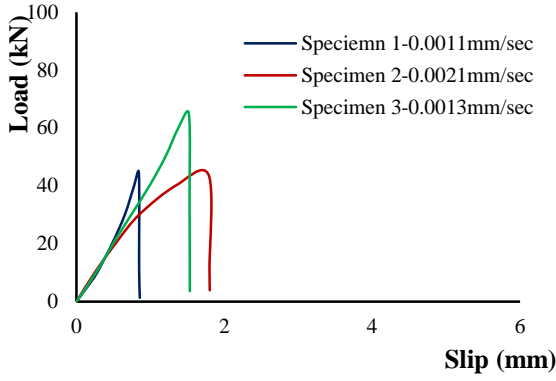


Figure 5: M30-0.5 Specimens (S1, S2, S3)

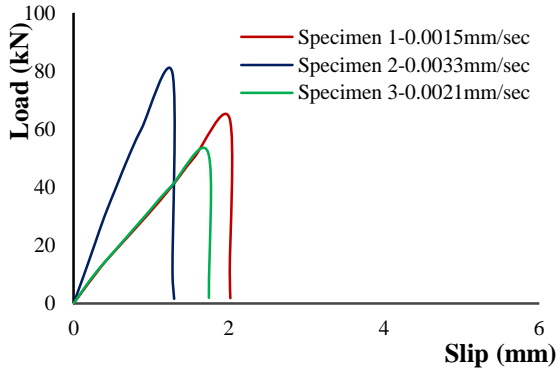


Figure 6: M70-0.32 Specimens (S1, S2, S3)

The load-slip response is linear up to the first cracking, then tends to become nonlinear up to the peak load followed by a sudden drop for all specimens. The peak load, P_{max} , and the ultimate/maximum slip, δ_{max} are shown in Table 2. Specimen M30-0.50-S3 failed along two shear planes as shown in Figure 3. From Figure 6, M70-0.32-S2 specimen taken more load compare to other two specimens, because the rate of displacement is higher compare to other specimens. The curves slightly vary in the linear portion up to peak load due to the variation of displacement rate.

5.4 Shear fracture toughness

The fracture toughness (K_{IIc}) of plain concrete in Mode II loading have been determined and are shown in Table 2. The area under the load-slip response was calculated, taken as the work of fracture. It is also called the toughness, W_{Fs} , in shear. The fracture energy per unit area in Mode II, G_{II} was computed using the following relationship

$$G_{II} = \frac{W_{Fs}}{2A_{eff}} \quad (1)$$

where A_{eff} is the effective area of cross section of the specimen at the failure plane.

The fracture toughness K_{IIc} was computed using the following equation

$$G_{II} = \frac{K_{IIc}(1 - \mu^2)}{E} \quad (2)$$

where E is the modulus of elasticity of concrete, equal to $5000\sqrt{f_{ck}}$ and μ is the Poisson's ratio 0.125 for concrete. In the above relationship, f_{ck} is concrete's average cube compressive strength. The fracture toughness, K_{IIc} values for two groups of plain concrete are 193.52 N/mm^{1.5} and 292.06 N/mm^{1.5}. Fracture energy (G_{II}) and fracture toughness (K_{IIc}) increase with increase in concrete's compressive strength.

5.5 Ultimate shear strength

The ultimate shear strengths of two groups of concretes have been computed by assuming an elastic response by the following formula

$$\tau = \frac{P_{max}}{2A_{eff}} \quad (3)$$

where P_{max} is the peak load on the specimen, and A_{eff} is the effective area of the cross-section. The average of three tests was considered for determining the shear strength of concrete. Where τ is shear strength in MPa; P is the maximum force in N; A_{eff} is the effective area of the cross-section = 120 x 120 = 14400 mm². The ultimate shear strength is reported in Table 2.

Table 2: Shear strength values of plain concrete

Specimen-Id	f_{ck} (MPa)	f_t	P_{max} kN	δ_{max} mm	τ_{max}	τ_{avg} MPa
M30-0.50-S1	32.89	2.89	44.53	0.86	1.55	1.53
M30-0.50-S2	31.83	2.69	43.67	1.78	1.52	
M30-0.50-S3	36.12	3.11	64.89	1.51	2.25	
M70-0.32-S1	72.84	4.77	63.71	2.22	2.22	2.25
M70-0.32-S2	75.46	5.42	79.33	2.75	2.75	
M70-0.32-S3	72.63	4.50	51.96	1.80	1.80	

M30-0.50-S3 failed along two shear planes, corresponding peak load and shear strength was more compared to other two specimens. The results showed a slight variation in the shear strength of concrete, which might be due to the inhomogeneity of concrete.

5.6 Fracture toughness vs. Compressive strength

As the compressive strength increases the fracture toughness also increases significantly. The failure in plain concrete was sudden and catastrophic

Table 3: Fracture parameters of plain concrete

Specimen-Id	$f_{ck\text{ avg}}$ (MPa)	W_{FS} N-m	G_{II} N/mm	K_{IIc} N/mm ^{1.5}	$K_{IIc\text{ avg}}$
M30-0.50-S1		16.01	0.56	128.96	
M30-0.50-S2	33.61	49.80	1.73	227.44	193.52
M30-0.50-S3		48.37	1.68	224.16	
M70-0.32-S1		65.39	2.38	314.45	
M70-0.32-S2	73.64	56.07	1.95	291.17	292.06
M70-0.32-S3		48.42	1.65	270.58	

6 CONCLUSIONS

A new test set-up has been developed to achieve shear failure to standardise. The following conclusions have been drawn.

1. The proposed test method generates a pure mode-II failure. All Specimens failed in brittle mode in shear with less warning before collapse along predefined plane.
2. The specimens were tested with different loading rates from 0.0011 to 0.0033 mm/sec. The rate of loading affects the peak load and fracture toughness, which shows that fracture toughness of concrete is influenced by the rate of loading.
3. The shear strength and fracture toughness increase with increase in concrete's compressive strength.
4. The fracture toughness increases with increase of fracture energy.

REFERENCES

[1] Barr, B., & Derradj, M., 1990. Numerical study of a shear (mode II) type test sp. geometry. *EFM*. **35**:(1–3), 171–180.

[2] Prakash Desayi; Raghuprasad B.K.; and Bhaskar Desai V., 1999. Mode II Fracture of Cementitious Materials – Part I: Studies on Specimens of Some New Geometries” *J. of Str Engg. (SERC)*, **Vol. 26**: pp. 11-18

[3] Proposki, G., 1991. Influence of water - cement ratio on micro-cracking of ordinary conc. *J. Mat. Sci.*, **26**: 6352–6356

[4] Amir A. Mirsayah; and Nemkumar Banthia, 2022. Shear Strength of Steel Fiber RC, *ACI Mat JI*, **V. 99**: pp. 473-479.

[5] Rao, G.A. and Rao, A.S., 2010. Toughness indices of fiber reinforced concrete subjected to mode II loading. *Proc. Fract. Mech. Concr. Struct.*, pp.112-117

[6] Appa Rao, G., & Sreenivasa Rao, A., 2009. Toughness indices of steel fiber reinforced concrete under mode II loading. *Mat. Str.*, **42(9)**:1173–1184

[7] Mu, R., Wang, Z., Wang, X., Qing, L., & Li, H., 2018. Experimental study on shear properties of aligned steel fiber reinforced cement-based comp. *CBM*. **184**:27–33

[8] Sadovskaya, E. A., Polonina, E. N., Leonovich, S. N., Zhdanok, S. A., & Potapov, V. V., 2022. Fracture Toughness of Nanofiber-Rein Concrete on Normal Separation and In-Plane Shear. *J. of Eng. Phy. and The.*, **95(4)**:945–952

[9] Qing, L., Sun, H., Zhang, Y., Mu, R., & Bi, M., 2023. Research progress on aligned fiber reinforced cement-based composites. *Const. and Build. Mat.*, **363**, p.129578

[10] JSCE-SF6., 1990. Method of test for shear strength of steel fiber reinforced concrete. *JSCE, Tokyo*, pp. 67–9

[11] Garcia, T., Blanco, A., & Cavalaro, S. H. P., 2016. Shear behaviour of sprayed concrete. *CBM*. **124**: 722–731